

Supporting Information: Brønsted-Acid-Catalyzed Exchange in Polyester Dynamic Covalent Networks

Jeffrey L. Self,[‡] Neil D. Dolinski,[‡] Manuel S. Zayas,[‡] Javier Read de Alaniz,[‡] and Christopher M. Bates^{||[‡],¹*}

[‡]Department of Chemistry and Biochemistry, ^{||}Materials Department, ¹Department of Chemical Engineering, University of California, Santa Barbara, Santa Barbara, California 93106, United States

Corresponding author:

* cbates@ucsb.edu

Experimental methods.....	3
Reagent and solvent information	3
Instrumentation	3
Synthesis	3
4-Methylcaprolactone (4mCL):	3
4,4'-Bioxepane-7,7'-dione (BOD):	3
Sample preparation	4
Figure S1. General process flow for sample preparation and testing.	4
Rheology procedure.....	4
Physical properties.....	5
Table S1. Physical properties of the Brønsted acid catalysts studied herein.*	5
Table S2. Glass transition temperature of select polymer networks.	5
Quantifying conversion.....	6
Solid state ¹³ C NMR: TCA.....	6
Figure S2. Solid state ¹³ C NMR spectrum of a polyester network containing TCA catalyst. Inset: magnification of the methyl resonance. Near quantitative conversion of the monomer is evidenced by the shift to lower frequency after polymerization.	6
Figure S3. The same solid state ¹³ C NMR spectrum as Figure S2 (TCA catalyst) demonstrates ≈96% conversion of the cross-linker.....	7
Solid state ¹³ C NMR: MSA	8
Figure S4. Solid state ¹³ C NMR spectrum of a polyester network containing MSA catalyst. Inset: magnification of the methyl resonance. Near quantitative conversion of the monomer is evidenced by the shift to lower frequency after polymerization.	8
Figure S5. The same solid state ¹³ C NMR spectrum as Figure S4 (MSA catalyst) demonstrates quantitative conversion of the cross-linker.	9
Figure S6. Select TCA normalized stress relaxation traces with model fit (white dashed lines) superimposed. Note the small y-axis range to better visualize the data.	10
Table S3. TCA fit parameters.....	10

Figure S7. Select MSA normalized stress relaxation traces with model fit (white dashed lines) superimposed.	11
Table S4. MSA fit parameters.	11
Figure S8. Select BSA normalized stress relaxation traces with model fit (white dashed lines) superimposed.	12
Table S5. BSA fit parameters.....	12
Figure S9. Select HTFSI normalized stress relaxation traces with model fit (white dashed lines) superimposed.	13
Table S6. HTFSI fit parameters.....	13
Figure S10. Select Triflic normalized stress relaxation traces with model fit (white dashed lines) superimposed.	14
Table S7. Triflic fit parameters.....	14
Rheology and fitting.....	15
Figure S11. Comparison of experimentally determined characteristic relaxation times to those calculated using the stretched exponential function shows good agreement.....	15
Table S8. Characteristic relaxation times, both empirically determined and those calculated from the fit model, with their respective relative residual errors.....	15
Amplitude sweep comparison	16
Figure S12. Comparison of moduli across different samples. The relative standard deviation is 21% for storage moduli and 76% for loss moduli.	16
Arrhenius analysis comparisons.....	16
Figure S13. Arrhenius plot from Figure 4a without vertical offsets.....	16
Figure S14. Four samples of MSA demonstrate reasonable reproducibility in the temperature range studied. Activation energies agree within 4% relative standard error (49 ± 2 kJ/mol) and the prefactors agree within 8% relative standard error (-9.1 ± 0.7).	17
Figure S15. Effect of MSA catalyst concentration on Arrhenius parameters.	17
Figure S16. MSA polyester networks are recyclable as expected for dynamic networks that undergo associative exchange.	18
Figure S17. The temperature-dependent relaxation behavior of MSA and BSA samples exhibits a cross-over at 52 °C (dashed line). This observation explains their similar characteristic relaxation times at the temperatures tested despite different Arrhenius parameters as reported in Figures 3b and 4.	19
References	20

Experimental methods

Reagent and solvent information

Reagents and solvents were used as received except where otherwise stated. Triflic acid (98%), benzenesulfonic acid (98%), methanesulfonic acid (HPLC grade, $\geq 99.5\%$), trichloroacetic acid ($\geq 99\%$) and 4-methylcyclohexanone ($\geq 99\%$) were purchased from Sigma-Aldrich. Tone 3031 (initiator) and 4,4'-bicyclohexanone ($>98\%$) were purchased from TCI America. Bistriflimide ($\geq 99\%$) and 3-chloroperoxybenzoic acid (70–75%) were purchased from Acros Organics. Dichloromethane (ACS grade, $\geq 99.5\%$) was purchased from Fisher Chemical and passed through activated alumina before use.

Instrumentation

Proton nuclear magnetic resonance (^1H NMR) spectra were collected using a 600 MHz Varian spectrometer. All chemical shifts (δ ppm) are reported relative to residual protio- CHCl_3 (7.26 ppm) in deuterated CDCl_3 . The ^{13}C solid state MAS NMR measurements were performed on a Bruker AVANCE III 500 MHz (11.7 T) wide bore spectrometer, operating at 500.24 MHz and 125.79 MHz for ^1H and ^{13}C , respectively, with a 4 mm zirconia rotor system at a spinning frequency of 10 kHz. The ^{13}C MAS experiments were performed with a 30 degree ^{13}C excitation pulse of 1.33 μs , a 3 s relaxation delay, a 80.9 ms acquisition time, and an accumulation of about 20,000 scans. 60 kHz proton decoupling was applied during ^{13}C data acquisition. The chemical shifts were referenced to a TMS standard. Parallel plate oscillatory rheology experiments were conducted on a TA Instruments AR-G2 magnetic bearing rheometer with a Peltier heating stage.

Synthesis

4-Methylcaprolactone (4mCL): The following procedure was adapted from Hillmyer et al.¹ In a typical reaction, a 500 mL round bottom flask was charged with a stir bar and 3-chloroperoxybenzoic acid (72 g, 321 mmol, 1.2 eq.). To this vessel was added dichloromethane (300 mL) while stirring. Due to impurities in the 3-chloroperoxybenzoic acid, an aqueous layer formed on top after complete dissolution, which was promptly removed. The reaction vessel was then degassed with a purge of Ar gas for 10 minutes while stirring and cooled to 0 °C. 4-Methylcyclohexanone (30 g, 267 mmol, 1.0 eq.) was added dropwise to the solution, which was left stirring for 16 hours. Thereafter, 100 mL of dichloromethane was added, followed by aqueous washes: 400 mL of 10% sodium bisulfite (2x), 400 mL of saturated sodium bicarbonate (2x), and saturated brine (1x). The organic layer was dried over magnesium sulfate and the solvent removed *in vacuo* to yield a colorless liquid. This crude product was distilled from calcium hydride to give 4-methylcaprolactone in 95% purity (23 g, 203 mmol) and 66% isolated yield. ^1H NMR (600 MHz, Chloroform-*d*) δ 4.22 (ddd, $J = 12.9, 5.8, 1.9$ Hz, 1H), 4.14 (dd, $J = 12.9, 10.4$ Hz, 1H), 2.60 (m, 2H), 1.89 (dt, $J = 15.3, 4.0$ Hz, 1H), 1.83 (m, 1H), 1.73 (m, 1H), 1.45 (dtd, $J = 15.3, 10.8, 1.9$ Hz, 1H), 1.28 (dtd, $J = 14.0, 11.3, 2.6$ Hz, 1H), 0.95 (d, $J = 6.6$ Hz, 3H).

4,4'-Bioxepane-7,7'-dione (BOD): The following procedure was adapted from Wiltshire et al.² In a typical reaction, a 250 mL round bottom flask was charged with a stir bar and 3-chloroperoxybenzoic acid (11 g, 46 mmol, 3 eq.). To this vessel was added dichloromethane (150 mL) while stirring. Due to impurities in 3-chloroperoxybenzoic acid, an aqueous layer formed on top after complete dissolution which was promptly removed. The reaction vessel was then degassed with a purge of Ar gas for 10 minutes while stirring and subsequently cooled to 0 °C. 4,4'-Bicyclohexanone (3.0 g, 15 mmol, 1 eq.) was dissolved in a minimal amount of dichloromethane, added dropwise to the solution, and the resulting solution was left stirring for 16 hours. Thereafter, 200 mL of dichloromethane was added to the solution, followed by

aqueous washes: 400 mL of 10% sodium bisulfite (2x), 400 mL of saturated sodium bicarbonate (4x), and saturated brine (1x). The organic layer was dried over magnesium sulfate and the solvent removed *in vacuo* to give 2.6 g of a white solid (26 g, 203 mmol) in 74% isolated yield with 97% purity. ^1H NMR (600 MHz, Chloroform-*d*) δ 4.33 (dd, $J = 5.1, 7.2$ Hz, 2H), 4.15 (dd, $J = 13.1, 9.2$ Hz, 2H), 2.72 (ddd, $J = 14.2, 7.4, 1.6$ Hz, 2H), 2.59 (ddt, $J = 14.5, 12.5, 2.3$ Hz, 2H), 1.89 (m, 2H), 1.84 (m, 2H), 1.4 (m, 4H), 1.48 (q, $J = 12.1$ Hz, 2H).

Sample preparation

A 1 dram vial was charged with the initiator Tone 3031 (0.035 g, 0.1 mmol, 1.0 eq.), 4mCL monomer (0.320 g, 2.5 mmol, 25 eq.), BOD cross-linker (0.068 g, 0.3 mmol, 3.0 eq.), and dichloromethane (0.2 mL) were sequentially added and the vial was sonicated until all reagents were completely dissolved. Finally, 1 stoichiometric equivalent of acid catalyst was added. For liquid catalysts, the acid was measured by micro-syringe and injected directly into the reaction vial. Conversely, for solid catalysts, the acid was first dissolved in 0.1 mL of dichloromethane and then added to the reaction vial. In both cases, the vial was rapidly shaken to ensure homogeneity and then left quiescent at room temperature for 20 hours to gel. Thereafter, the dram vials were broken and the polyester gel was gently removed. The gel was then subjected to a flow of argon for 1 hour to promote evaporation of residual dichloromethane and then annealed on a hot block at 75 °C. To ensure the correct geometry for characterization experiments, the sample was pressed into a round 8 mm aluminum mold template using a C-clamp and small aluminum top plate. The sample was left annealing at 75 °C for 4 hours before being removed and immediately loaded on the rheometer for testing. For samples containing TCA and MSA, excess material was removed by hand and submitted for solid state ^{13}C NMR analysis to quantify conversion. This process is depicted graphically below in Figure S1.

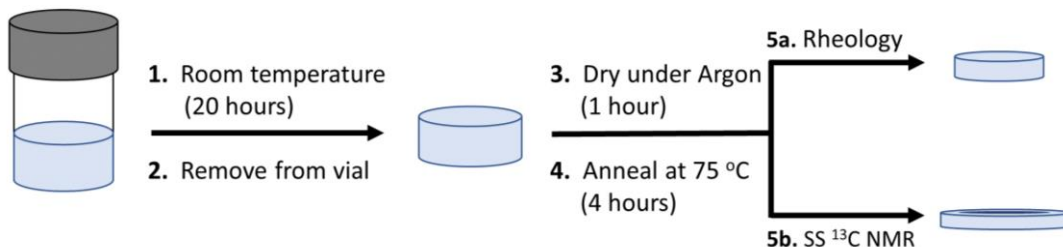


Figure S1. General process flow for sample preparation and testing.

Rheology procedure

A typical rheology sample was approximately 8 mm in diameter and 2 mm thick. These were loaded on an AR-G2 at a normal force of 1 N using an 8 mm parallel plate geometry. Active conditioning was used to produce a constant normal force (1.1 ± 0.1 N) by automatically adjusting the gap, which ensures similar testing conditions between each sample and at each temperature (across all samples the gap was only adjusted on the order of 200 microns over the entire experiment). Amplitude sweeps were collected for each sample to determine the appropriate strain amplitude within the linear viscoelastic regime. Stress relaxation data for all samples were collected at 0.5% strain and a frequency of 10 rads/s. The relaxation modulus was monitored for various amounts of time (e.g., 10,800 sec) depending on the sample. Several heating and cooling procedures were tested, which had minimal impact on the subsequent Arrhenius analysis.

Physical properties

Table S1. Physical properties of the Brønsted acid catalysts studied herein.*

Acid	Molar Mass (g/mol)	pK _a	Melting point (°C)	Boiling point (°C)	ρ (g/cm ³)
TCA	163.4	0.81	57–58	196	1.63
MSA	96.10	–1.9	20.	167	1.48
BSA	158.2	–7.0	51	190.	1.32
HTFSI	281.2	–9.7	46–57	91.0	1.36
Triflic	150.1	–12	–40.	162	1.70

*Data compiled from the following references: TCA,^{3,4} MSA,^{3,5} BSA,^{3,6} HTFSI,^{3,7} Triflic.^{3,8}

Table S2. Glass transition temperature of select polymer networks.

Acid	T _g (°C)
TCA	–55
MSA	–52
BSA	–56

Quantifying conversion
Solid state ^{13}C NMR: TCA

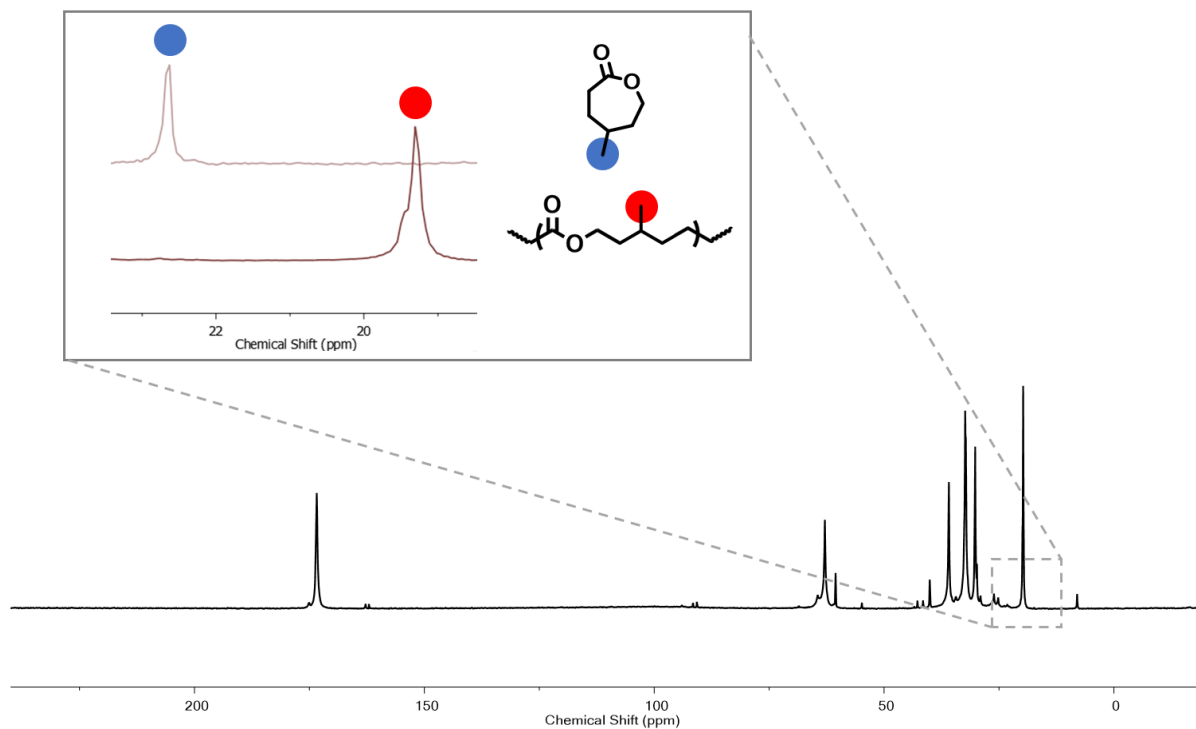


Figure S2. Solid state ^{13}C NMR spectrum of a polyester network containing TCA catalyst. Inset: magnification of the methyl resonance. Near quantitative conversion of the monomer is evidenced by the shift to lower frequency after polymerization.

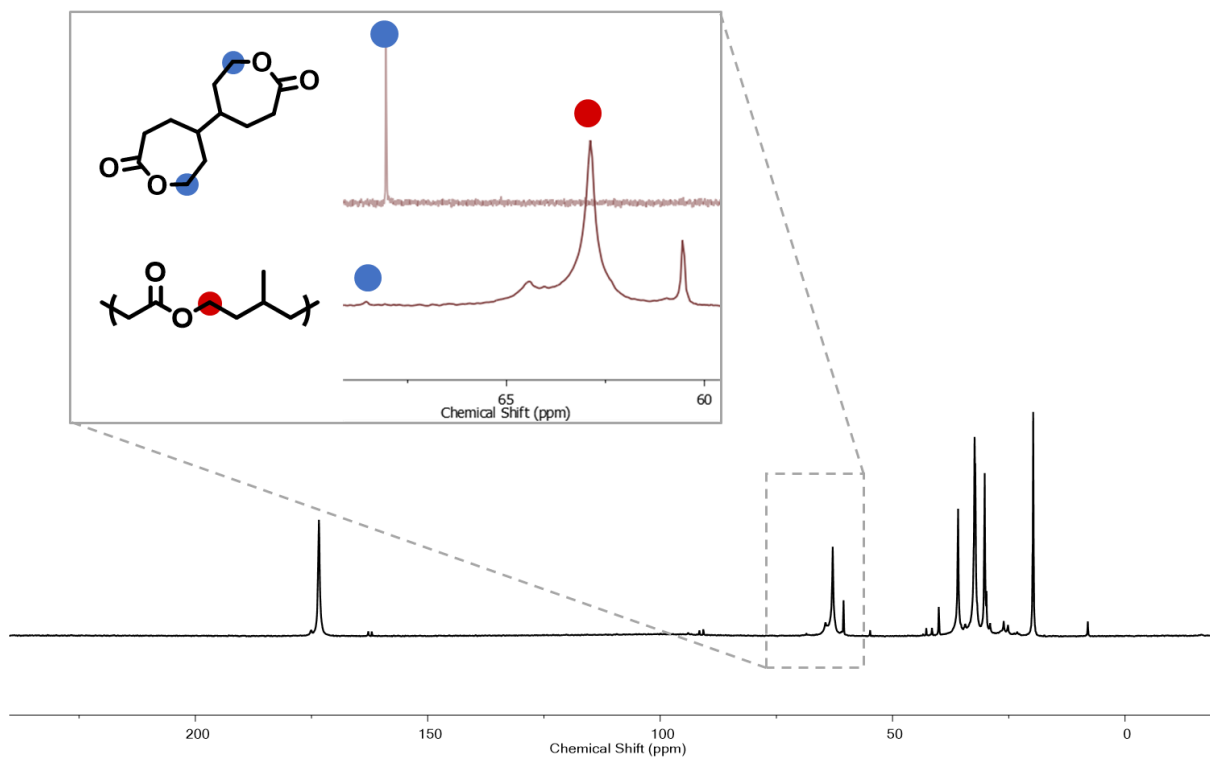


Figure S3. The same solid state ^{13}C NMR spectrum as Figure S2 (TCA catalyst) demonstrates $\approx 96\%$ conversion of the cross-linker.

Solid state ^{13}C NMR: MSA

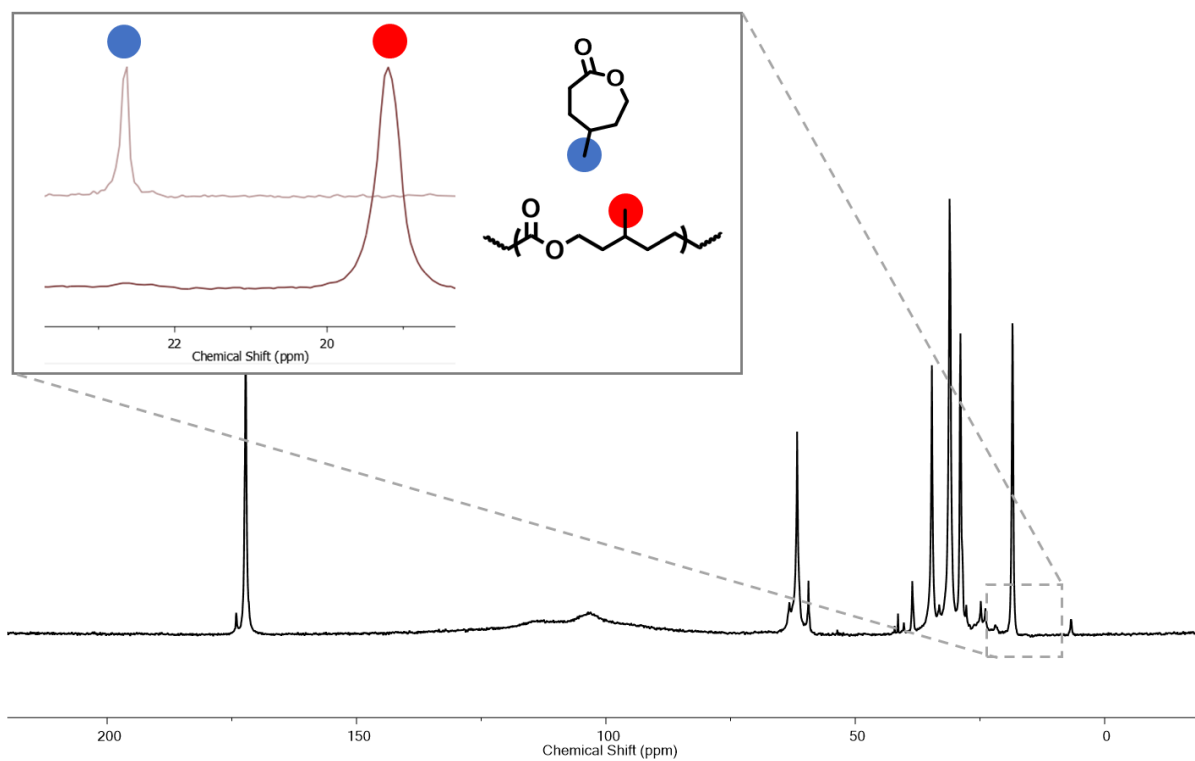


Figure S4. Solid state ^{13}C NMR spectrum of a polyester network containing MSA catalyst. Inset: magnification of the methyl resonance. Near quantitative conversion of the monomer is evidenced by the shift to lower frequency after polymerization.

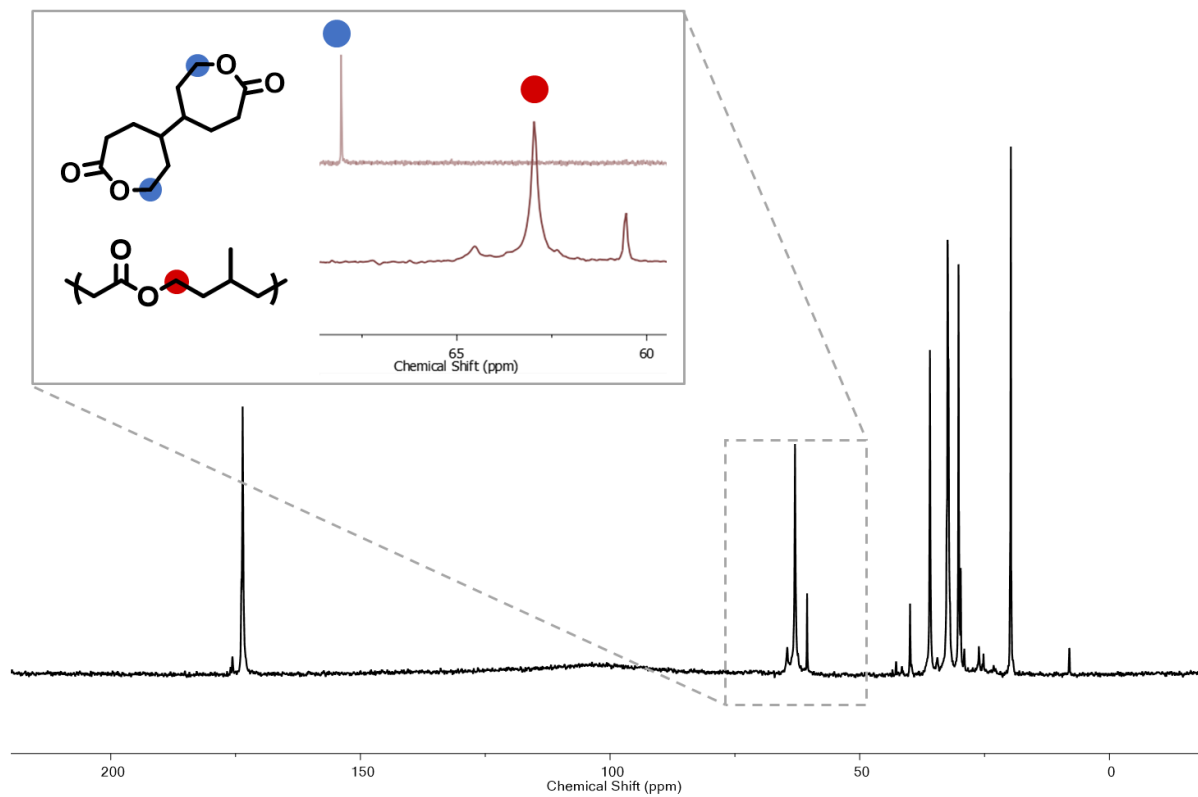


Figure S5. The same solid state ^{13}C NMR spectrum as Figure S4 (MSA catalyst) demonstrates quantitative conversion of the cross-linker.

Rheology and fitting: TCA

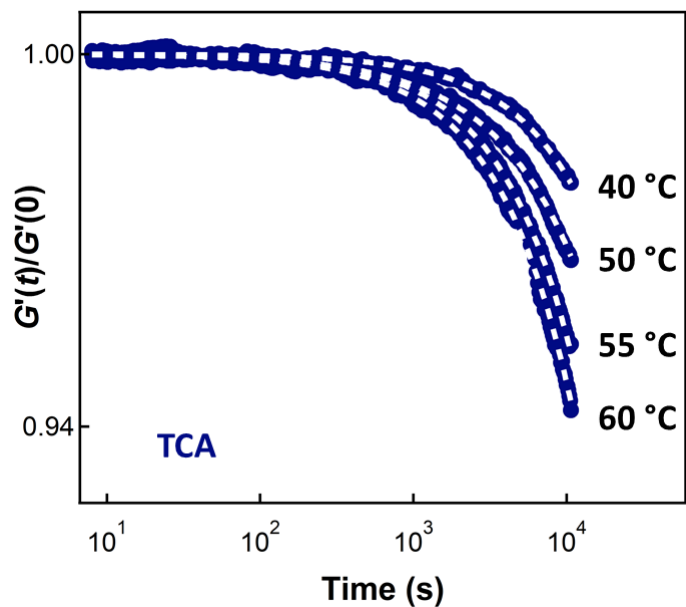


Figure S6. Select TCA normalized stress relaxation traces with model fit (white dashed lines) superimposed. Note the small y-axis range to better visualize the data.

Table S3. TCA fit parameters.

Run #	T (°C)	$(RT)^{-1}$	$\tau^* \times 10^{-5}$ (s)	$\ln \tau^*$	α
1	45	0.378	7.71	13.6	0.79
2	55	0.367	3.00	12.6	0.90
3	60	0.361	2.71	12.5	0.88
4	50	0.372	4.31	13.0	0.91
5	40	0.384	7.09	13.5	0.92

Rheology and fitting: MSA

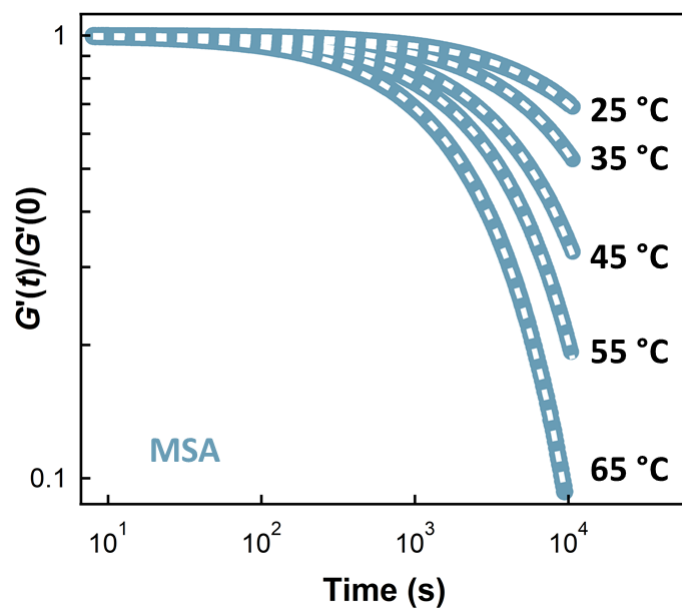


Figure S7. Select MSA normalized stress relaxation traces with model fit (white dashed lines) superimposed.

Table S4. MSA fit parameters.

Run #	T (°C)	$(RT)^{-1}$	$\tau^* \times 10^{-3}$ (s)	$\ln \tau^*$	α
1	45	0.378	9.04	9.11	0.80
2	35	0.391	18.0	9.80	0.82
3	55	0.367	5.62	8.63	0.81
4	25	0.404	34.9	10.5	0.83
5	65	0.356	3.30	8.10	0.82

Rheology and fitting: BSA

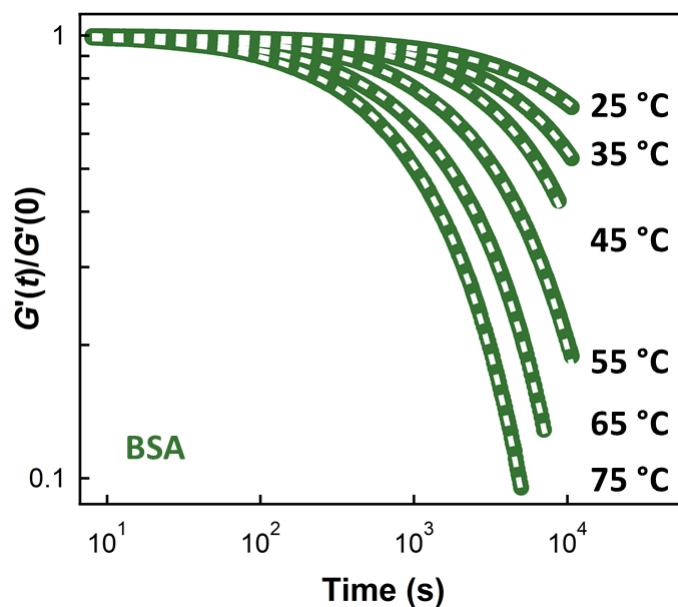


Figure S8. Select BSA normalized stress relaxation traces with model fit (white dashed lines) superimposed.

Table S5. BSA fit parameters.

Run #	T (°C)	$(RT)^{-1}$	$\tau^* \times 10^{-3}$ (s)	$\ln \tau^*$	α
1	35	0.391	19.3	9.87	0.77
2	55	0.367	5.36	8.59	0.78
3	75	0.346	1.65	7.41	0.78
4	65	0.356	2.77	7.93	0.77
5	25	0.404	43.9	10.7	0.72
6	45	0.378	10.3	9.23	0.83

Rheology and fitting: HTFSI

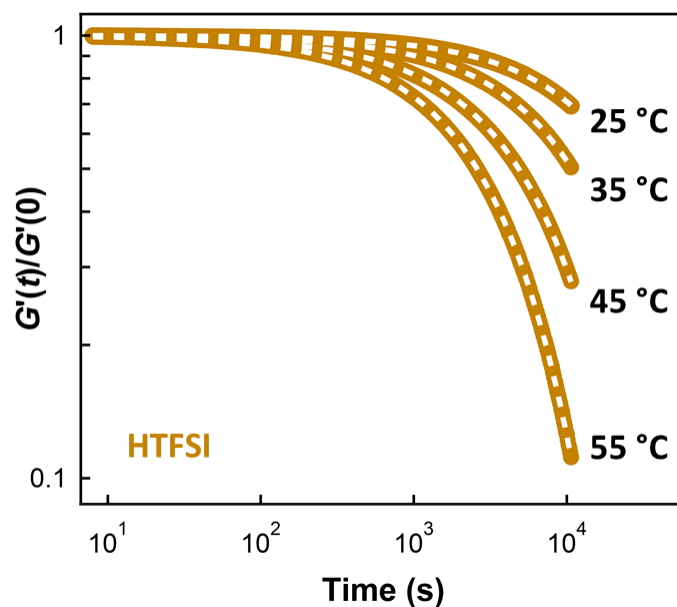


Figure S9. Select HTFSI normalized stress relaxation traces with model fit (white dashed lines) superimposed.

Table S6. HTFSI fit parameters.

Run #	T (°C)	$(RT)^{-1}$	$\tau^* \times 10^{-3}$ (s)	$\ln \tau^*$	α
1	55	0.367	4.07	8.31	0.81
2	45	0.378	7.77	8.96	0.78
3	35	0.391	17.1	9.74	0.80
4	25	0.404	36.7	10.52	0.82

Rheology and fitting: Triflic acid

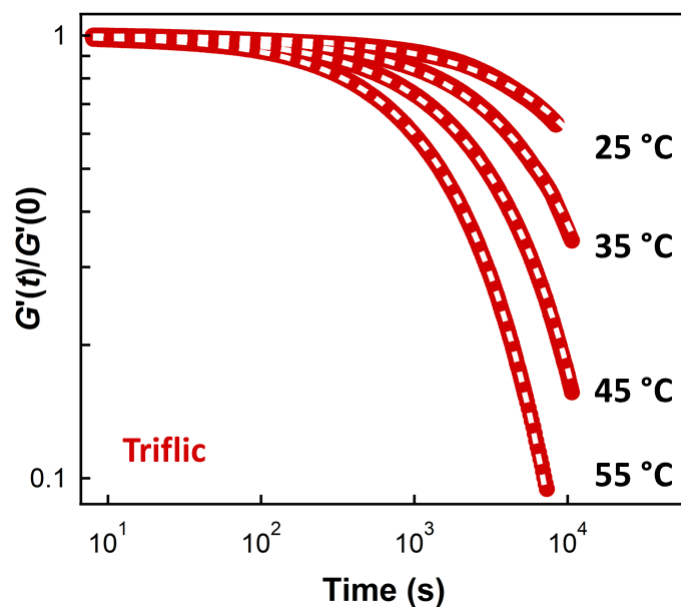


Figure S10. Select Triflic normalized stress relaxation traces with model fit (white dashed lines) superimposed.

Table S7. Triflic fit parameters.

Run #	T (°C)	$(RT)^{-1}$	$\tau^* \times 10^{-3}$ (s)	$\ln \tau^*$	α
1	55	0.367	2.36	7.77	0.78
2	45	0.378	4.77	8.47	0.75
3	35	0.391	10.3	9.24	0.74
4	25	0.404	26.9	10.2	0.72

Rheology and fitting

To evaluate the utility of the fit model, we empirically determined τ^* values for those samples that sufficiently relaxed (to at least $G'(t)/G'(0) = e^{-1}$) and compared them to those predicted by fits to the stretched exponential function. Since the results show excellent agreement (Figure S11), analyses described in the text and below were carried out with fit τ^* values, even for samples that did not relax enough to measure an experimental τ^* .

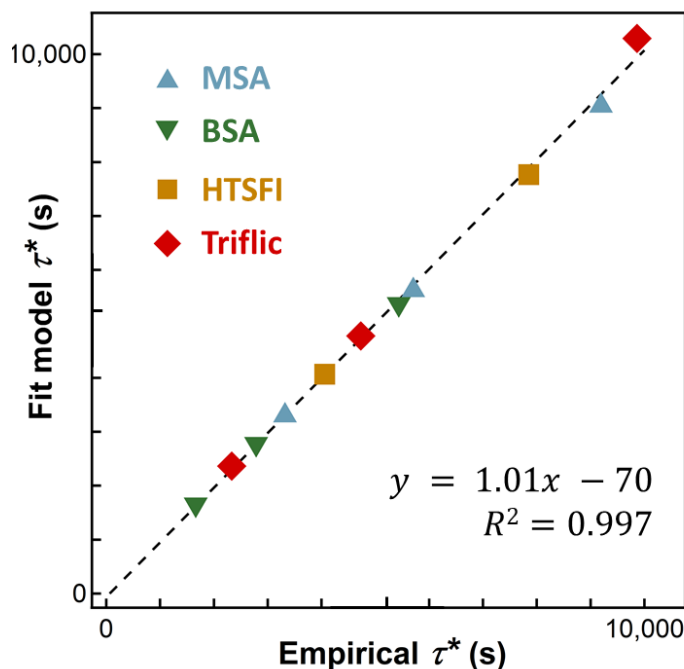


Figure S11. Comparison of experimentally determined characteristic relaxation times to those calculated using the stretched exponential function shows good agreement.

Table S8. Characteristic relaxation times, both empirically determined and those calculated from the fit model, with their respective relative residual errors.

Acid	T (°C)	τ^*		% error
		Experimental (s)	Fit model (s)	
Triflic	35	9,865	10,290	-4.3
	45	4,731	4,774	-0.9
	55	2,332	2,363	-1.3
HTFSI	45	7,852	7,767	1.1
	55	4,060.	4,065	-0.1
BSA	55	5,436	5,367	1.3
	65	2,785	2,773	0.4
	75	1,661	1,652	0.5
MSA	45	9,194	9,040.	1.7
	55	5,704	5,623	1.4
	65	3,322	3,299	0.7

Amplitude sweep comparison

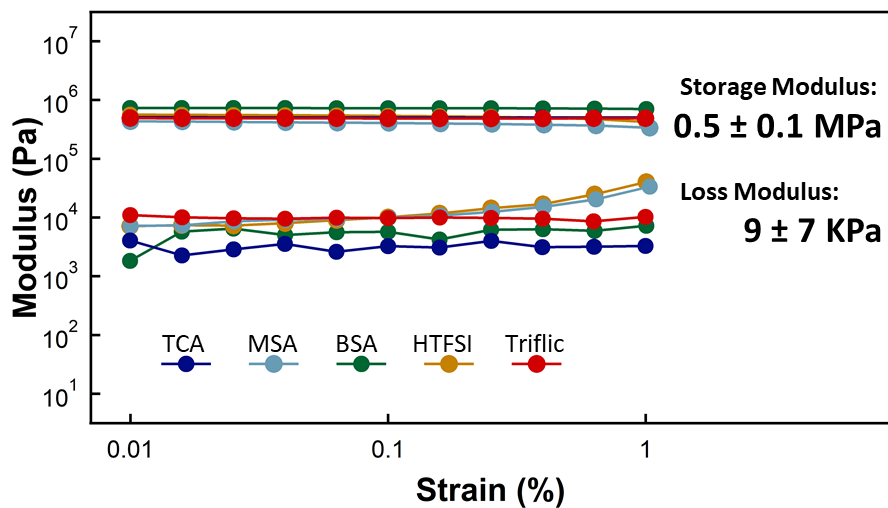


Figure S12. Comparison of moduli across different samples. The relative standard deviation is 21% for storage moduli and 76% for loss moduli.

Arrhenius analysis comparisons

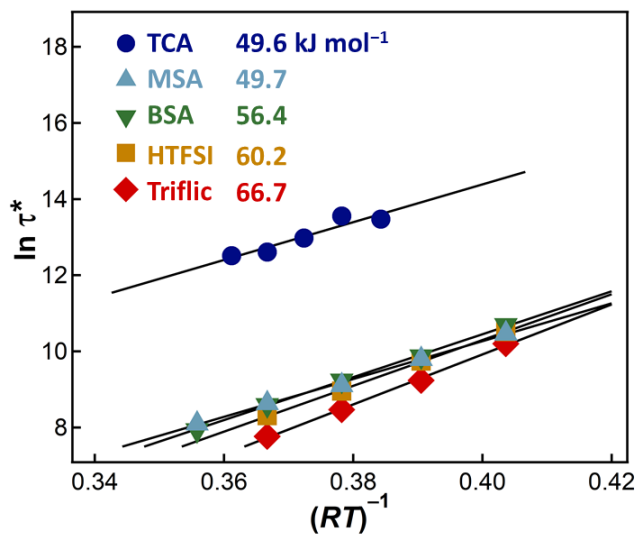


Figure S13. Arrhenius plot from Figure 4a without vertical offsets.

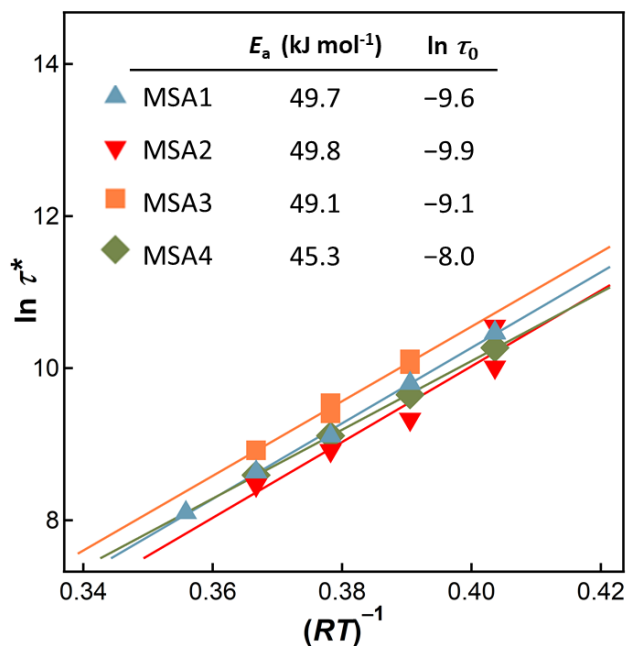


Figure S14. Four samples of MSA demonstrate reasonable reproducibility in the temperature range studied. Activation energies agree within 4% relative standard error (49 ± 2 kJ/mol) and the prefactors agree within 8% relative standard error (-9.1 ± 0.7).

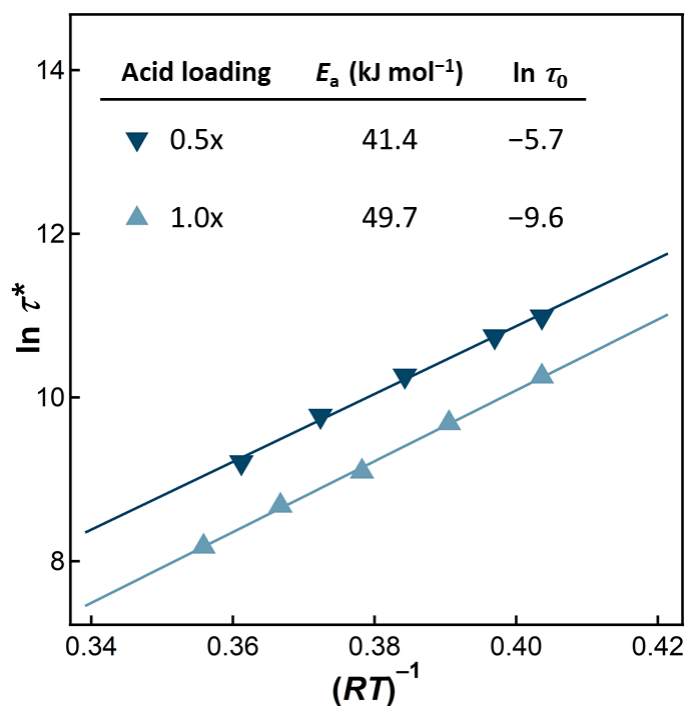


Figure S15. Effect of MSA catalyst concentration on Arrhenius parameters.

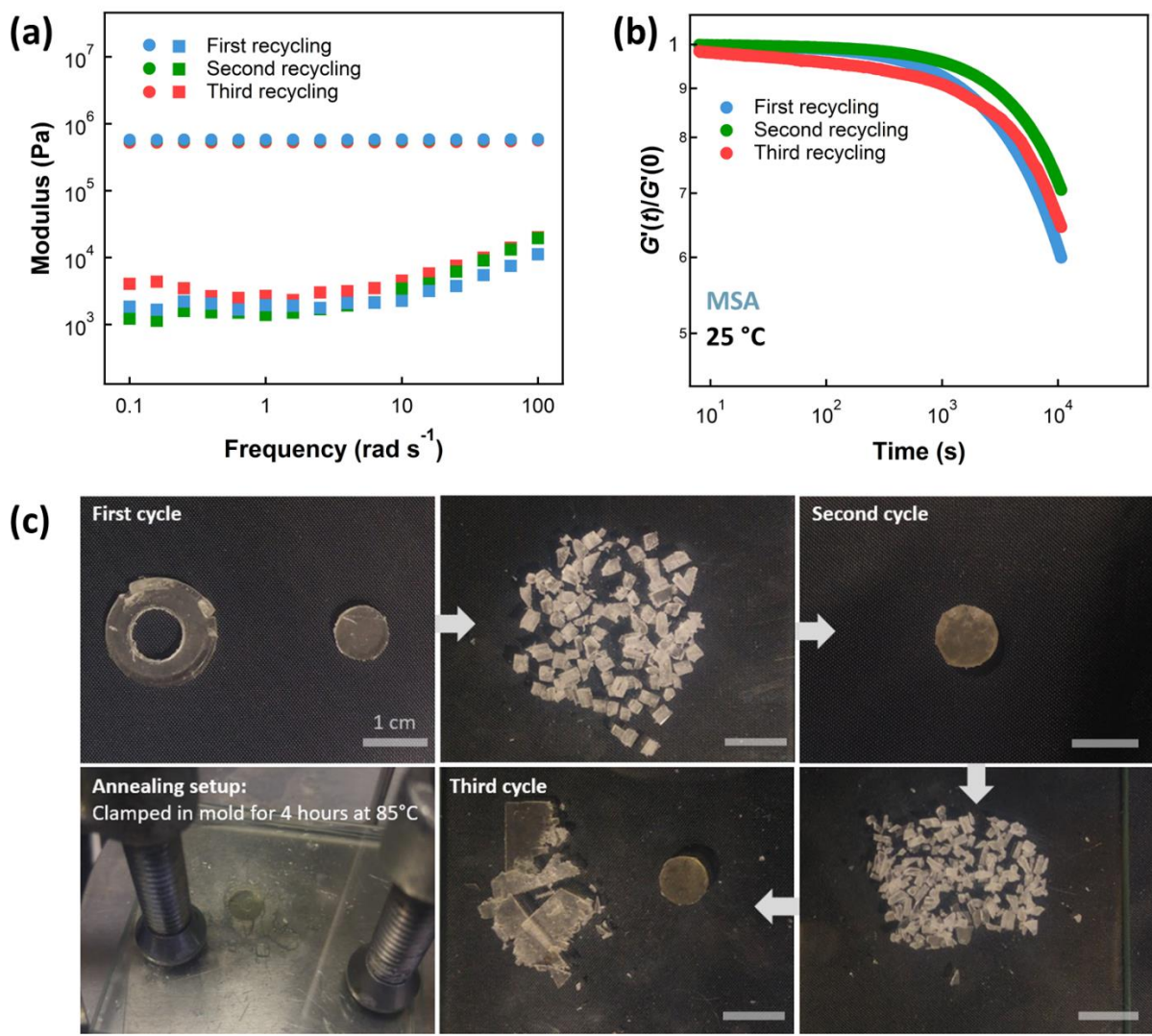


Figure S16. MSA polyester networks are recyclable as expected for dynamic networks that undergo associative exchange.

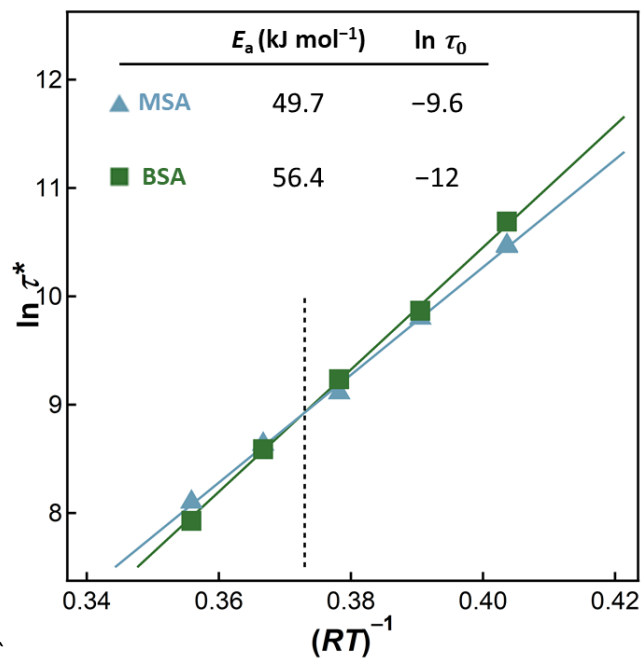


Figure S17. The temperature-dependent relaxation behavior of MSA and BSA samples exhibits a cross-over at 52 °C (dashed line). This observation explains their similar characteristic relaxation times at the temperatures tested despite different Arrhenius parameters as reported in Figures 3b and 4.

References

- (1) Watts, A.; Kurokawa, N.; Hillmyer, M. A. Strong, Resilient, and Sustainable Aliphatic Polyester Thermoplastic Elastomers. *Biomacromolecules* **2017**, *18* (6), 1845–1854. DOI: 10.1021/acs.biomac.7b00283
- (2) Wiltshire, J. T.; Qiao, G. G. Degradable Core Cross-Linked Star Polymers via Ring-Opening Polymerization. *Macromolecules* **2006**, *39* (13), 4282–4285. DOI: 10.1021/ma060712v
- (3) Kim, S.; Thiessen, P. A.; Bolton, E. E.; Chen, J.; Fu, G.; Gindulyte, A.; Han, L.; He, J.; He, S.; Shoemaker, B. A.; Wang, J.; Yu, B.; Zhang, J.; Bryant, S.H. PubChem Substance and Compound Databases. *Nucleic Acids Res.* **2016**, *44* (D1), D1202–D1213. DOI: 10.1093/nar/gkv951
- (4) Shroff, R.; Rulisek, L.; Doubsky, J.; Svatos, A. Acid-Base-Driven Matrix-Assisted Mass Spectrometry for Targeted Metabolomics. *Proc. Natl. Acad. Sci. U. S. A.* **2009**, *106* (25), 10092–10096. DOI: 10.1073/pnas.0900914106
- (5) Luong, B. X.; Petre, A. L.; Hoelderich, W. F.; Commarieu, A.; Laffitte, J. A.; Espeillac, M.; Souchet, J. C. Use of Methanesulfonic Acid as Catalyst for the Production of Linear Alkylbenzenes. *J. Catal.* **2004**, *226* (2), 301–307. DOI: 10.1016/j.jcat.2004.05.025
- (6) Shamir, D.; Zilbermann, I.; Maimon, E.; Shames, A. I.; Cohen, H.; Meyerstein, D. Anions as Stabilizing Ligands for Ni(III)(Cyclam) in Aqueous Solutions. *Inorganica Chim. Acta* **2010**, *363* (12), 2819–2823. DOI: 10.1016/j.ica.2010.03.057
- (7) Paenurk, E.; Kaupmees, K.; Himmel, D.; Kütt, A.; Kaljurand, I.; Koppel, I. A.; Krossing, I.; Leito, I. A Unified View to Brønsted Acidity Scales: Do We Need Solvated Protons? *Chem. Sci.* **2017**, 6964–6973. DOI: 10.1039/C7SC01424D
- (8) Raamat, E.; Kaupmees, K.; Ovsjannikov, G.; Trummal, A.; Kütt, A.; Saame, J.; Koppel, I.; Kaljurand, I.; Lipping, L.; Rodima, T.; Pihl, V.; Koppel, I.; Leito, I. Acidities of Strong Neutral Brønsted Acids in Different Media. *J. Phys. Org. Chem.* **2013**, *26* (2), 162–170. DOI: 10.1002/poc.2946